

Date Palm Stones as an Eco-Friendly Natural Adsorbent for Basic Blue 41 Dye Removal from Wastewater: Batch Adsorption Study

Shatha Salim Taresh¹

¹General Directorate of Education in Dewania, Ministry of Education, Iraq.

Publication Date: 2026/06/12

Abstract

Discharge of textile effluents containing synthetic dye is still one of the more obstinate environmental challenges in many developing locations. The present work has focused on the investigation of raw date palm (*Phoenix dactylifera*) stones, which are an abundant agricultural by-product in Iraq, as a low-cost natural adsorbent for the removal of Basic Blue 41 (BB41), a cationic azo dye, from aqueous solution. The material was not subjected to any chemical or thermal activation, only washed, dried, powdered and sieved below 125 μm . FTIR, XRD and FESEM were used to evaluate the surface and structural properties and the point of zero charge was determined to be close to 6.3. Batch studies were conducted to investigate the effect of solution pH, adsorbent dose, contact time, initial dye concentration and temperature. The removal increased significantly with pH from 2 to \sim 8. This is consistent with electrostatic interaction between the protonated dye and the more negative biosorbent surface. Equilibrium was reached in around 75 min and uptake increased with increasing temperature. The kinetics data were better fit by the pseudo second order model and the equilibrium data by the Langmuir isotherm with a maximal monolayer capacity of about 48 mg/g. Thermodynamic analysis showed a positive value of ΔH° (about +21.5 kJ/mol) and negative values of ΔG° indicating an endothermic and spontaneous process. The results show that untreated date palm stones could be used as a real low-cost and practical adsorbent for waste water containing cationic dyes, while valorising a waste stream.

➤ Highlights

- Raw, unmodified date palm stone powder was used to adsorb Basic Blue 41 dye.
- No chemical or thermal activation was applied, which keeps the process low-cost.
- Adsorption followed pseudo-second-order kinetics and the Langmuir isotherm.
- The maximum monolayer capacity reached about 48 mg/g at the optimum conditions.
- The process was endothermic, spontaneous and driven mainly by electrostatic attraction.

Keywords: *Date Palm Stone; Basic Blue 41; Adsorption; Natural Adsorbent; Adsorption Isotherm; Thermodynamics; Wastewater Treatment.*

I. INTRODUCTION

Synthetic dyes are created and used in large quantities in the textile, leather, paper and food industries and a large proportion of this colour ends up in wastewater [1]. Apart from the obvious visual nuisance, many of these chemicals are poisonous, mutagenic or carcinogenic and their persistence in water interferes with light penetration and with the photosynthetic activity of aquatic systems [2].

Basic Blue 41 (BB41) is a mono-azo cationic dye extensively used for dyeing acrylic fibres. Like other azo dyes, it is resistant to ordinary biological treatment and its release into receiving waters poses a real hazard for aquatic life [3]. Various physico-chemical approaches have been employed to treat dye effluents such as coagulation, membrane filtration, advanced oxidation, electrochemical techniques etc. But most of the techniques have been hampered by high operating costs or generation of secondary waste. Adsorption is characterised by its simple operation, its flexibility and its capacity to provide

treated water of excellent quality [4]. Cationic dyes are particularly susceptible to severe colouration and visibility even at trace levels and their efficient removal has significance [5]. This has led to several modified carbons and other sorbents being investigated [6].

However, the high cost of commercial activated carbon often limits the application of adsorption in low-income settings, and this has led to a protracted quest for cheaper replacements from agricultural leftovers [7]. Date palm (*Phoenix dactylifera*) is cultivated extensively in the Middle East and North Africa, and Iraq produces enormous quantities of date stones as a processing by-product annually. Several authors have transformed these stones into activated carbon for dye and pollutant uptake [8, 9]. Most of them utilise chemical activation using chemicals such as zinc chloride [10]. Much less reported is the behaviour of the raw unactivated material which would circumvent the energy and chemical demands of activation altogether. Therefore, this work investigates raw date palm stone powder as a natural adsorbent for BB41. The specific objectives are to characterise the material, explore the key operating factors in batch mode and analyse the process using kinetic, isotherm and thermodynamic models.

II. MATERIALS AND METHODS

➤ *Chemicals and Adsorbate*

Basic Blue 41 (C.I. 11105; C₂₀H₂₆N₄O₆S₂; Molar mass: ~ 482.6 g/mol) was purchased commercially and utilised as received. A stock solution of 1000 mg/L was made by dissolving the needed amount of dye in distilled water. Working solutions were made by appropriate dilution from the stock solution. The absorbance of BB41 was greatest at about 608 nm and this wavelength was utilised throughout for the determination of concentrations with a UV-visible spectrophotometer. The pH of the solutions was changed using dilute HCl and NaOH.

➤ *Preparation of the Adsorbent*

Date palm stones were acquired locally and cleaned from any clinging meat. The stones were washed many times with tap water and then with distilled water to remove dust and soluble materials. The cleaned stones were dried in an oven at 70 °C for 24 h, and crushed and processed in a mill. The obtained powder was sieved and the fraction under 125 µm was used for all the experiments. There was no chemical or thermal activation. The material was used as it is and kept in a closed container until use.

➤ *Characterization*

Fourier-transform infrared (FTIR) spectroscopy was used to identify the functional groups of the adsorbent before and after dye uptakes in the range of 4000–400cm⁻¹. X-ray diffraction (XRD) was used to study the crystalline or amorphous nature of the powder. Field-emission scanning electron microscopy (FESEM) was used to evaluate the surface morphology. These approaches are usually utilised to correlate surface structure with adsorption behaviour on carbon based and

lignocellulosic adsorbents [11, 12]. The point of zero charge (pH_{pzc}) was determined using the salt-addition (pH-drift) method. For this, a series of 0.1 M NaCl solutions were prepared with beginning pH values from 2 to 10, a set amount of adsorbent was added to each and the final pH was recorded after 24 h. pH_{pzc} is the pH at which the starting and final values are the same.

➤ *Batch Adsorption Procedure*

Batch experiments were performed by agitating a known mass of adsorbent with 50 mL of dye solution of known concentration in a series of conical flasks on a shaker at room temperature, unless stated otherwise. At the end of the contact period the suspensions were filtered and the residual dye concentration in the supernatant was measured spectrophotometrically. The amount of dye adsorbed at equilibrium, q_e (mg/g), and the removal efficiency (%) were calculated from the usual mass-balance relationships [13]:

$$q_e = (C_0 - C_e) V / m \quad (1)$$

$$\text{Removal (\%)} = [(C_0 - C_e) / C_0] \times 100 \quad (2)$$

where C₀ and C_e are the initial and equilibrium dye concentrations (mg/L), V is the volume of solution (L) and m is the mass of adsorbent (g).

➤ *Effect of Operating Variables*

The effect of solution pH was studied over the range 2–10 at a fixed dye concentration and dose. The adsorbent dosage was varied from 0.5 to 5 g/L, the initial BB41 concentration from 10 to 100 mg/L, and the contact time from a few minutes up to equilibrium. Temperature effects were examined at 298, 308 and 318 K. Each run was carried out with the other conditions held constant, so that the influence of one variable could be isolated at a time.

➤ *Adsorption Modelling*

• *Kinetic Models.*

The rate of BB41 uptake was analysed with the pseudo-first-order [14], pseudo-second-order [15] and intraparticle diffusion [16] models, written respectively as:

$$\ln(q_e - q_t) = \ln q_e - k_1 t \quad (3)$$

$$t / q_t = 1 / (k_2 q_e^2) + t / q_e \quad (4)$$

$$q_t = k_{id} t^{0.5} + C \quad (5)$$

where q_t is the amount adsorbed at time t (mg/g); k₁ (1/min), k₂ (g/mg·min) and k_{id} (mg/g·min^{0.5}) are the corresponding rate constants; and C (mg/g) is related to the thickness of the boundary layer.

• *Isotherm Models.*

Equilibrium data were fitted to the Langmuir [17], Freundlich [18], Temkin [19] and Dubinin–Radushkevich [20] isotherms:

$$C_e / q_e = 1 / (q_{max} K_L) + C_e / q_{max} \quad (6)$$

$$RL = 1 / (1 + KL C_0) \quad (7)$$

$$\ln q_e = \ln KF + (1/n) \ln C_e \quad (8)$$

$$q_e = B \ln KT + B \ln C_e \quad (9)$$

$$\ln q_e = \ln q_m - \beta \varepsilon^2 \quad (10)$$

$$\varepsilon = R T \ln(1 + 1/C_e); \quad E = 1 / \sqrt{(2\beta)}$$

where q_{max} is the maximum monolayer capacity (mg/g), KL the Langmuir constant (L/mg), RL the dimensionless separation factor, KF and n the Freundlich constants, KT (L/g) and B the Temkin constants, β the D-R activity coefficient and E the mean free energy of adsorption (kJ/mol).

- *Thermodynamic Parameters.*

The thermodynamic quantities were obtained from the variation of the distribution coefficient with temperature:

$$\Delta G^\circ = - R T \ln K_c \quad (11)$$

$$\ln K_c = \Delta S^\circ / R - \Delta H^\circ / (R T)$$

where K_c is the equilibrium constant, R the gas constant (8.314 J/mol·K) and T the absolute temperature (K). ΔH° and ΔS° were obtained from the slope and

intercept, respectively, of the van't Hoff plot of $\ln K_c$ against $1/T$.

III. RESULTS AND DISCUSSION

➤ Characterization of the Adsorbent

The FTIR spectrum of the raw date palm stone powder (Fig. 1a) showed a broad band centred near 3400 cm^{-1} , assigned to O–H stretching of hydroxyl groups belonging to cellulose, hemicellulose and lignin and overlapping with adsorbed moisture. A weaker absorption around 2920 cm^{-1} corresponded to C–H stretching of aliphatic methyl and methylene groups. The band near 1740 cm^{-1} was attributed to C=O stretching of carbonyl and carboxyl functions, while the feature close to 1620 cm^{-1} is usually associated with C=C stretching of aromatic rings and with bound water. Several overlapping bands between 1050 and 1250 cm^{-1} arose from C–O and C–O–C stretching of the polysaccharide skeleton. This collection of oxygen-containing groups is exactly what one would expect from an untreated lignocellulosic material, and it offers a range of potential binding sites for a cationic dye. After BB41 adsorption a number of these bands shifted by a few wavenumbers and lost intensity, the O–H and C=O regions being the most affected; such changes are a reasonable sign that hydroxyl and carboxyl groups take part in dye binding. The detailed assignments before and after adsorption are collected in Table 1.

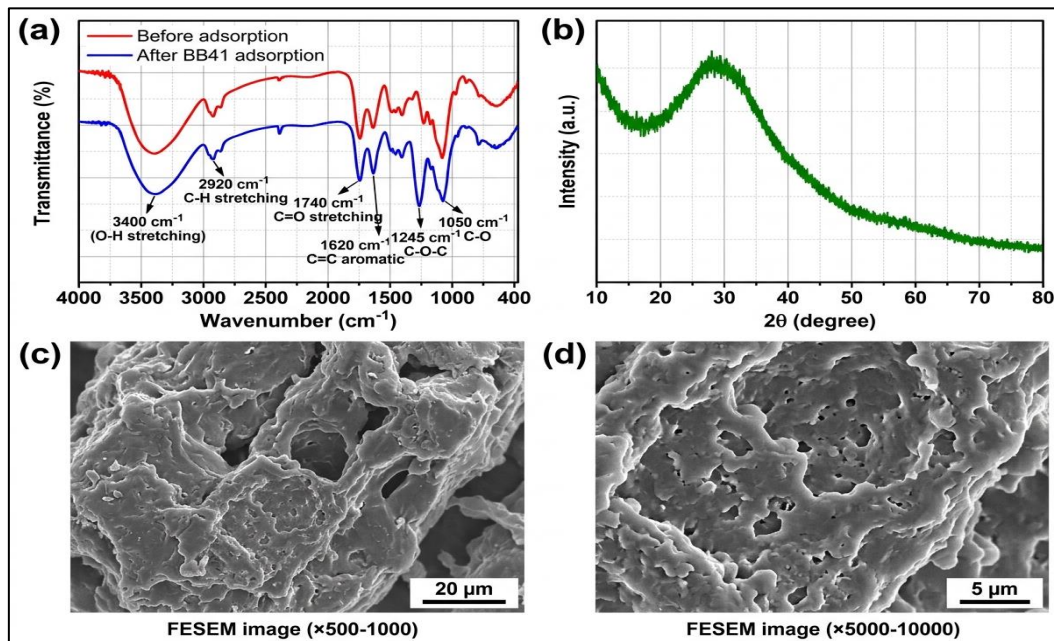


Fig 1 Characterisation of the Raw Date Palm Stone Adsorbent: (a) FTIR Spectra before and after the BB41 Adsorption, (b) XRD pattern, (c) FESEM Picture at low Magnification, and (d) FESEM Image at high Magnification

Table 1 FTIR Band Allocations of the Date Palm Stone Before and After Adsorption of BB41.

Functional group / vibration	Before adsorption (cm ⁻¹)	After adsorption (cm ⁻¹)	Change after adsorption
O–H stretching (hydroxyl)	3400	3415	Broadened, intensity reduced (major)
C–H stretching (aliphatic)	2920	2916	Slight shift
C=O stretching (carbonyl)	1740	1728	Shifted, intensity reduced (major)
C=C aromatic / adsorbed H ₂ O bnding	1620	1614	Slight shift
C–O–C asymmetric stretching	1245	1240	Minor shift
C–O stretching	1050	1046	Minor shift

The X-ray diffraction pattern (Fig. 1b) showed a broad, diffuse hump instead of distinct peaks, which means that the powder is mostly amorphous with only short-range crystalline organization. This is the typical hallmark of lignocellulosic biomass without carbonised or chemically treated [11]. FESEM micrographs (Fig. 1c, d) showed an irregular and somewhat rough surface with the presence of cavities, folds and channels of varying diameters. While the material does not exhibit the regular, highly developed pore network that would be produced by activation, this naturally heterogeneous texture does give a useful number of accessible sites for dye molecules to adhere to [12]. Overall, the characterization results depict a chemically well-equipped but structurally disordered surface, which is compatible with the moderate adsorption capacity demonstrated here.

The point of zero charge calculated by the pH-drift approach was close to 6.3. At solution pH values below this figure the surface is positively charged on balance, and increasingly negatively charged above it. It will become apparent that this single feature is the key to understanding the pH response of BB41 adsorption.

➤ *Effect of pH*

Solution pH is one of the most influential variables in dye adsorption, because it governs both the surface charge of the adsorbent and the form in which the dye exists in solution. The removal of BB41 by date palm stone powder was low under strongly acidic conditions and rose steadily as the pH increased from 2 to about 8, after which it levelled off (Fig. 2a). At low pH the abundance of H⁺ ions and the net positive surface charge — recall that the pHPzc lies near 6.3 — set up an electrostatic repulsion with the cationic dye, and protons also compete for the available binding sites. As the pH climbs past the pHPzc the surface turns negative, and the electrostatic attraction between the deprotonated surface and the positively charged BB41 molecules becomes the dominant interaction; the result is a clear improvement in uptake. A similar trend, in which cationic dye removal increases with rising pH, has been reported for many agricultural and carbon-based adsorbents. Beyond pH 8 the gain in removal was only marginal, so a value of about 8 was taken as optimal and adopted in the subsequent experiments. It is easy in practice to operate in the somewhat alkaline range, since many practical textile effluents are inherently alkaline.

➤ *Effect of Adsorbent Dosage*

The number of accessible binding sites, and consequently the extent of removal, is governed by the amount of adsorbent added to a fixed volume of dye solution. The percentage of BB41 eliminated rose significantly as the dose was increased from 0.5 to 5 g/L mainly because a bigger surface area and a higher number of active sites were provided to the same amount of dye (Fig. 2b). The rise was steep initially and then began to level off; above about 2 g/L, the additional removal obtained per unit mass was minimal. This plateau can

normally be explained in terms of two elements. First, at greater doses some sites are not occupied, simply because there is not enough dye in solution to fill them all. Second, particle aggregation can occur with high solid loading, leading to the decrease of effective surface area due to the overlapping of adsorption sites. The same pattern indicates the equilibrium absorption per gram, q_e , tends to decrease with increasing dose although the overall percentage elimination increases. For the remaining work a dose of around 2 g/L was chosen for a balance between efficient colour removal and economical use of the substance..

➤ *Effect of Contact Time and Initial Dye Concentration*

The evolution of BB41 adsorption with time followed a now recognised two-stage trajectory (Fig. 2c). The uptake was high during the first 15-20 min when the majority of the vacant surface sites were freely available and tapered down as these sites filled reaching a plateau at 75 min. This contact time was taken as the equilibrium point and was used in the equilibrium and thermodynamic runs. The curve form, a rapid initial sorption, followed by slow approach to saturation, is typical of adsorption on heterogeneous biomass surfaces and has been documented for numerous plant-derived adsorbents for the removal of cationic dyes [21].

The effect of initial dye concentration was studied in the range 10–100 mg/L (Fig. 2d). With increasing concentration the % removed fell slightly and amount absorbed per gram increased. The first observation is a result of the fixed number of binding sites. As the binding sites reach saturation fewer of the now bigger dye population can be accommodated. The second shows the part played by concentration as an engine. The higher initial concentration will create a larger gradient between the bulk solution and the surface, which will help the dye molecules overcome the resistance to mass transfer, and push more of them towards the adsorbent. These two effects are usually observed in dye-adsorption research, and they are really different ways of looking at the same equilibrium. From a treatment point of view, the drop in percentage removal at high loading suggests that very concentrated effluents would need either a higher dose or a staged operation to obtain an acceptable level of decolourisation.

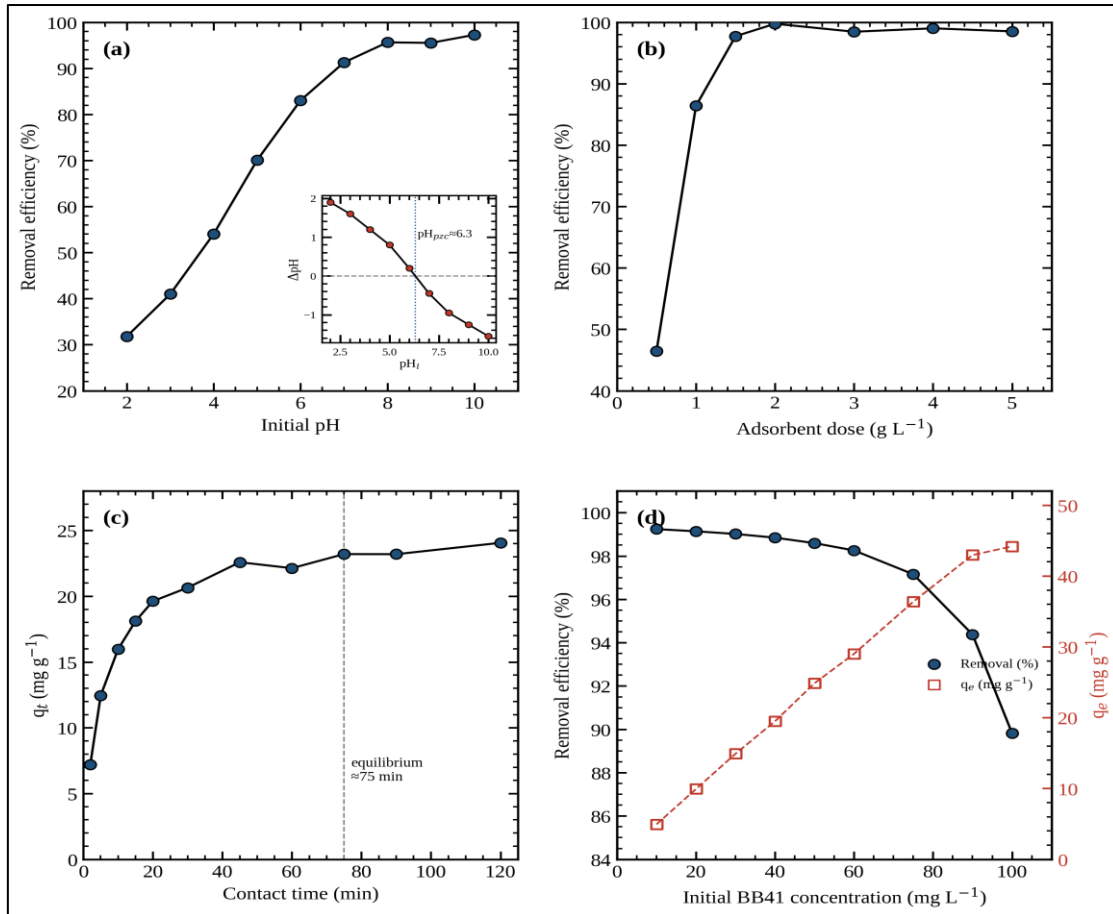


Fig 2 Effect of Operating Conditions on BB41 Elimination by Date Palm Stone Powder: (A) Solution pH (Inset Shows Determination of [pH_{pzc}]), (B) Dose of Adsorbent, (C) Length of Contact and (D) Initial Concentration of Dye.

➤ Adsorption kinetics

The time-course data were fitted to three kinetic models to get insight into the rate-controlling stages. The pseudo-first-order equation fitted only moderately when plotted as $\ln(q_e - q_t)$ versus t and the equilibrium capacity predicted by it deviated significantly from the measured one (Fig. 3a). The pseudo-second-order model performed considerably better: the plot of t/q_t versus t was highly linear, the correlation coefficient exceeded 0.99, and the

calculated q_e agreed closely with the experimental figure (Fig. 3b). On this basis the adsorption of BB41 onto date palm stone powder is best described as pseudo-second order, which is usually taken to mean that chemisorption involving valence forces, or the sharing of electrons between the dye and surface groups, contributes to the rate-limiting step. The same conclusion has been drawn for a wide range of low-cost carbons and biosorbents [22]. The fitted kinetic parameters are listed in Table 2.

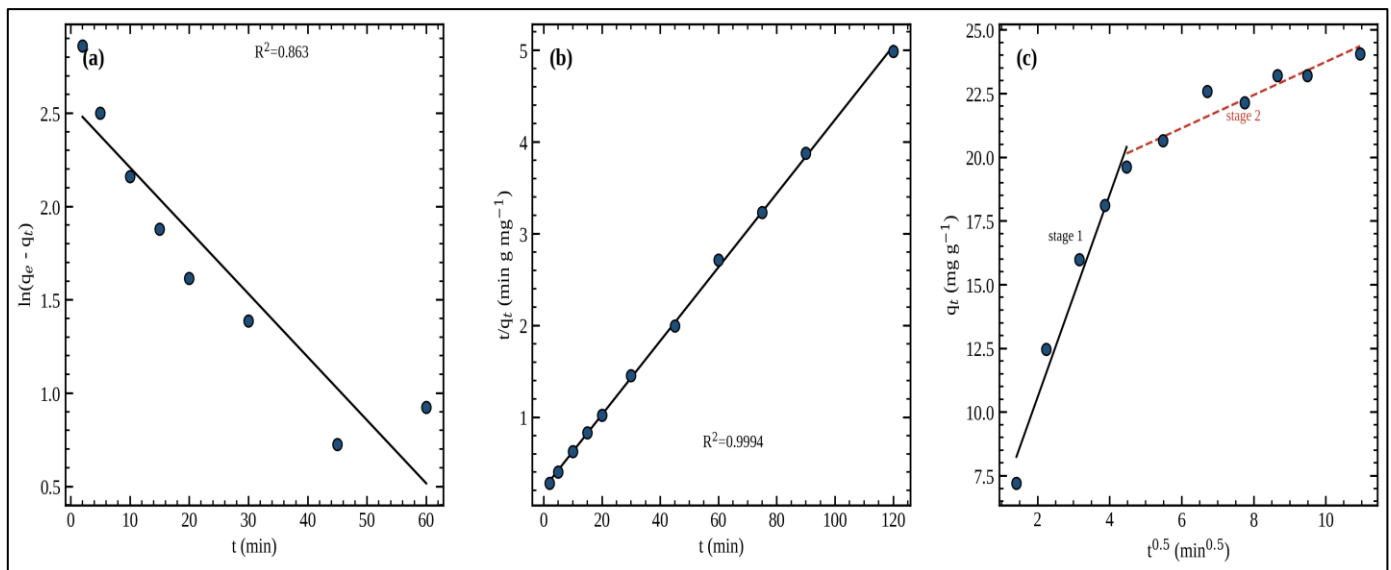


Fig 3 Adsorption Kinetics of BB41 onto Date Palm Stone Powder: (A) Pseudo-First-Order, (B) Pseudo-Second-Order, and (C) Intraparticle Diffusion (Weber–Morris) Plots.

Table 2 Kinetic Parameters For BB41 Adsorption (Pseudo-First-Order, Pseudo-Second-Order And Intraparticle Diffusion Models).

Kinetic model	Parameters	R ²
Pseudo-first-order	$q_{e,cal} = 12.78 \text{ mg g}^{-1}$; $k_1 = 0.0339 \text{ min}^{-1}$	0.863
Pseudo-second-order	$q_{e,cal} = 24.88 \text{ mg g}^{-1}$ ($q_{e,exp} = 24.06 \text{ mg g}^{-1}$); $k_2 = 7.30 \times 10^{-3} \text{ g mg}^{-1} \text{ min}^{-1}$; $h = 4.52 \text{ mg g}^{-1} \text{ min}^{-1}$	0.9994
Intraparticle diffusion — stage 1	$k_{id1} = 3.97 \text{ mg g}^{-1} \text{ min}^{-0.5}$; $C_1 = 2.62 \text{ mg g}^{-1}$	0.968
Intraparticle diffusion — stage 2	$k_{id2} = 0.65 \text{ mg g}^{-1} \text{ min}^{-0.5}$; $C_2 = 17.23 \text{ mg g}^{-1}$	0.895

The intraparticle diffusion model was then used to test whether diffusion within the particles controls the process (Fig. 3c). The plot of qt against $t^{0.5}$ was not a single straight line passing through the origin but instead showed two or more linear segments, the first steeper than the next. This multi-linear behaviour suggests more than one operating mechanism with a first stage dominated by external mass transfer or boundary layer diffusion to the outer surface and a slower stage of sluggish diffusion into the internal cavities. None of the segments travelled through the origin, which means that the intraparticle diffusion is involved but is not the only rate determining step. Surface adsorption together with film diffusion also clearly plays a contribution..

➤ Adsorption Isotherms

Equilibrium isotherms connect the amount of dye retained on the surface to the concentration remaining in solution and are crucial both to predicting capacity and to understanding the nature of the interaction. Four classical models were tested here. The Langmuir isotherm, which assumes monolayer coverage on a surface of energetically uniform sites, gave the best description of the data, with a correlation coefficient close to unity (Fig. 4a). The maximum monolayer capacity, q_{max} , derived from this model was about 48 mg/g under the conditions studied. The dimensionless separation factor RL fell between 0 and 1 across the whole concentration range, confirming that the adsorption is favourable. A comparable preference for the Langmuir model has been reported for BB41 removal by several inorganic and natural sorbents [23].

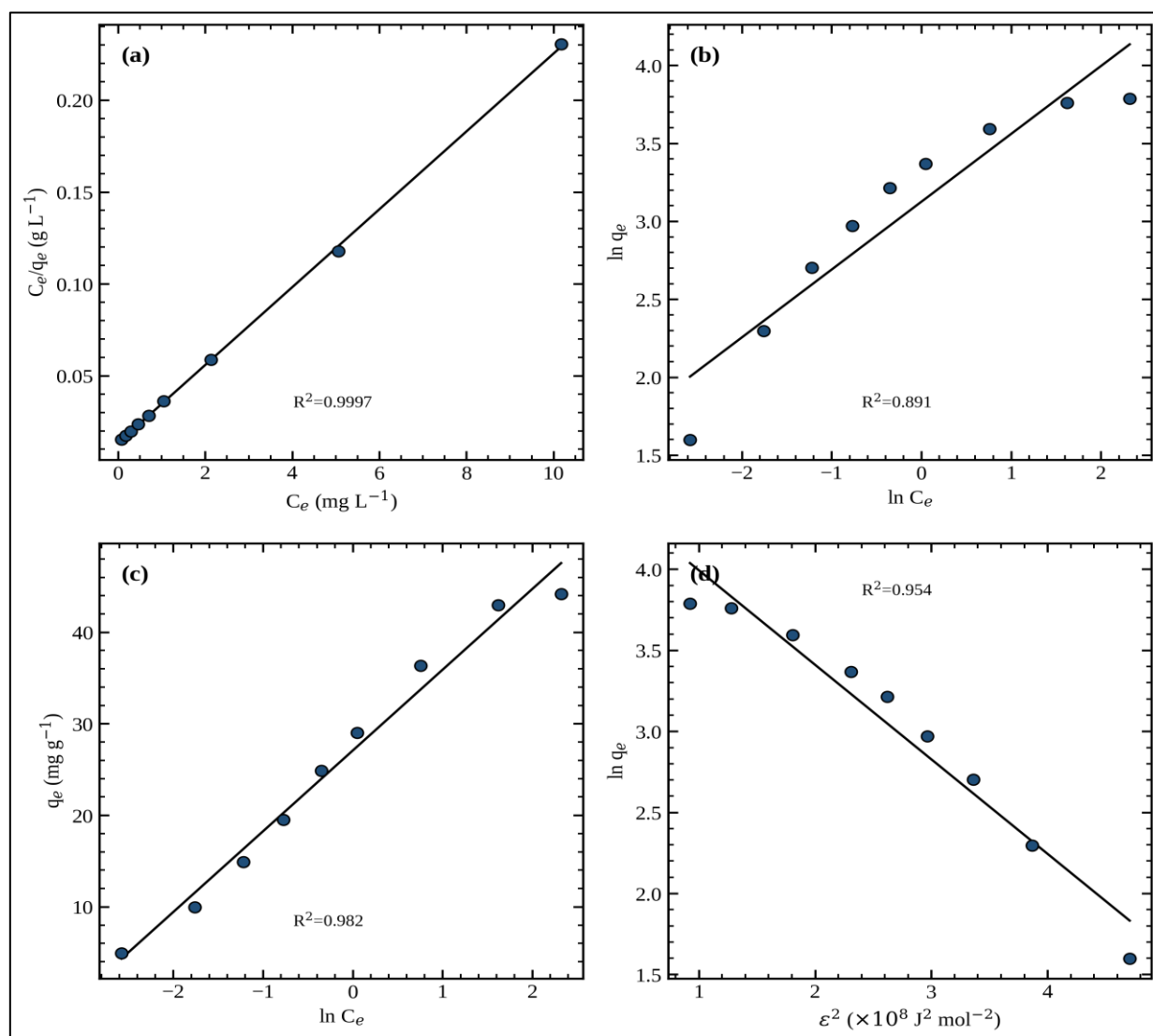


Fig 4 Equilibrium Isotherms for Bb41 Adsorption onto Date Palm Stone Powder: (A) Langmuir, (B) Freundlich, (C) Temkin, And (D) Dubinin–Radushkevich Models.

Table 3 Isotherm parameters for BB41 adsorption (Langmuir, Freundlich, Temkin and Dubinin–Radushkevich models).

Isotherm model	Parameters	R ²
Langmuir	$q_{\max} = 47.21 \text{ mg g}^{-1}$; $K_L = 1.574 \text{ L mg}^{-1}$; $R_L = 0.006\text{--}0.060$	0.9997
Freundlich	$K_F = 22.77 (\text{mg g}^{-1})(\text{L mg}^{-1})^{1/n}$; $n = 2.30$; $1/n = 0.435$	0.891
Temkin	$K_T = 21.49 \text{ L g}^{-1}$; $B = 8.83 \text{ J mol}^{-1}$; $b_T = 280.7 \text{ J mol}^{-1}$	0.982
Dubinin–Radushkevich	$q_m = 97.2 \text{ mg g}^{-1}$; $\beta = 5.83 \times 10^{-9} \text{ mol}^2 \text{ J}^{-2}$; $E = 9.26 \text{ kJ mol}^{-1}$	0.954

The Freundlich model, which describes adsorption on heterogeneous surfaces with a distribution of site energies, also fitted reasonably well, and the value of $1/n$ was less than one, again pointing to a favourable process (Fig. 4b). The fact that both Langmuir and Freundlich give acceptable fits is not unusual for biomass adsorbents, whose surfaces combine relatively uniform and heterogeneous regions; this is consistent with the chemically mixed surface revealed by FTIR. The Temkin isotherm (Fig. 4c) provided a measure of the adsorption energy and supported the presence of moderate adsorbent–dye interactions, in line with reports on date-derived carbons used for cationic dyes [24].

Finally, the Dubinin-Radushkevich model (Fig. 4d) was used to estimate the mean free energy of adsorption, E . The measured value in the region of 9–10 kJ/mol is close to the boundary frequently used to differentiate physical from chemical adsorption, indicating a mixed character process where both physical forces and weaker chemical interactions contribute. Similar border-line energies have been obtained for dye adsorption on lignocellulosic adsorbents made from date palm residues [25]. The entire collection of isotherm constants is shown in Table 3.

➤ *Effect of Temperature and Thermodynamic Study*

The effect of temperature was studied at 298, 308 and 318 K (Fig. 5a). The removal of BB41 was improved with

increasing temperature which instantly speaks of an endothermic mechanism. Higher temperatures can contribute to adsorption in more than one way at the same time: kinetic energy increases in the dye molecules facilitating their diffusion to the surface; the viscosity of the solution decreases; and the minor swelling of the biomass might expose a few more active sites.

The thermodynamic parameters were obtained from the temperature data by van't Hoff technique (Fig. 5b). The enthalpy change, ΔH° , was positive at about +21.5 kJ/mol, indicating the endothermic character of adsorption. The rise in entropy, $\Delta S^\circ = +78 \text{ J/mol.K}$, indicates an increase in disorder at the solid-solution interface as the dye binds, which is generally due to the liberation of water molecules that had been organised around the dye and the surface. The Gibbs free energy change, ΔG° , was negative at all three temperatures, ~ -1.74, -2.52 and -3.30 kJ/mol at 298, 308 and 318 K respectively, and it got increasingly negative with increasing temperature. This suggests that the adsorption is spontaneous and more thermodynamically favourable at higher temperatures. The size of ΔH° is consistent with the borderline physical-chemical character implied by the D-R energy, confirming the concept that the uptake is not governed only by strong chemical bonding. These parameters are listed in Table 4.

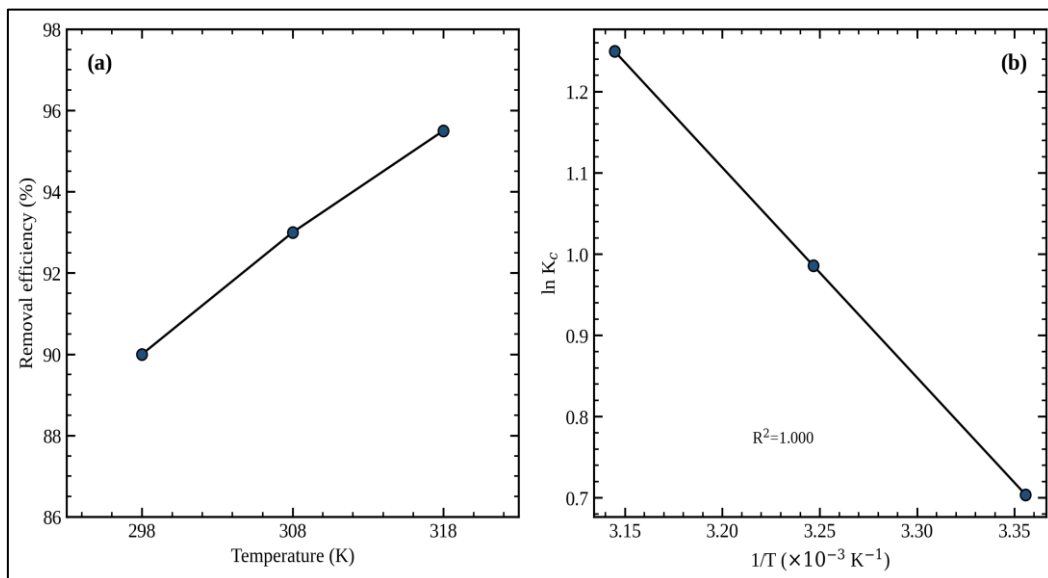


Fig 5 Effect of Temperature and Thermodynamics of BB41 Adsorption onto Date Palm Stone Powder: (A) Effect of Temperature on Removal Efficiency, and (B) Van't Hoff Plot of Ln Kc Against 1/T.

Table 4 Thermodynamic parameters for BB41 adsorption at different temperatures.

T (K)	K _c	$\Delta G^\circ (\text{kJ mol}^{-1})$	$\Delta H^\circ (\text{kJ mol}^{-1})$	$\Delta S^\circ (\text{J mol}^{-1} \text{K}^{-1})$
298	2.02	-1.74	+21.50	+78.0
308	2.68	-2.52		
318	3.49	-3.30		

To place these results in context, the maximum capacity of the raw date palm stone powder was compared with that of other low-cost adsorbents reported for BB41 and related cationic dyes (Table 5). Activated and chemically modified materials generally reach higher capacities, as one would expect, but the untreated stones still offer a respectable uptake without any activation step — which is the main practical attraction of the present approach.

Table 5 Comparison of Maximum Adsorption Capacity (Q_{max}) Of Date Palm Stone Powder with Other Low-Cost Adsorbent Reported For Basic Blue 41 and Other Comparable Cationic Dyes.

Adsorbent	Target dye	q_{max} (mg g ⁻¹)	Reference
Persea americana nut activated carbon (H ₃ PO ₄ activated)	BB41	625	[4]
Date palm stone powder (raw, unmodified)	BB41	47.21	This study
Date stones (raw biomass)	Methylene Blue	43.47	[7]
Palm-trees waste (raw biomass)	Methylene Blue	39.47	[7]
Hydroxysodalite zeolite (from Jordanian kaolin)	BB41	39	[23]
Juniperus excelsa shavings powder	BB41	16.53	[3]

IV. CONCLUSION

This study aims to evaluate the potential of raw and unmodified date palm stones as a practical adsorbent for the cationic dye (Basic Blue 41) and the findings obtained were promising. The grinding stones removed a significant portion of BB41 from aqueous solution without any chemical or heat activation. The performance was mainly controlled by solution pH. FTIR confirmed the presence of a mixture of oxygen-containing surface groups, whereas XRD and FESEM revealed a rough and mostly amorphous structure. The fastest uptake was in the first 20 min or so and equilibrium was attained about 75 min following pseudo second order kinetics. The equilibrium results were best fitted by the Langmuir isotherm with a maximum monolayer capacity of roughly 48 mg/g. The thermodynamic analysis indicated that the process was endothermic, spontaneous and accompanied by an increase in entropy. The main interaction seems to be an electrostatic attraction between the negatively charged surface and the cationic dye, promoted by surface hydroxyl and carboxyl groups. Due to its abundance, very cheap cost and absence of any activation phase, date palm stone powder is a promising natural adsorbent for the treatment of dye-bearing wastewater and needs additional research on real effluents and in continuous-flow systems.

REFERENCES

- [1]. Tkaczyk A, Mitrowska K, Posyniak A. Synthetic organic dyes as contaminants of the aquatic environment and their implications for ecosystems: a review. *Science of the Total Environment*. 2020;717:137222.
- [2]. Al-Tohamy R, Ali SS, Li F, Okasha KM, Mahmoud YA-G, Elsamahy T, et al. A critical review on the treatment of dye-containing wastewater: ecotoxicological and health concerns of textile dyes and possible remediation approaches for environmental safety. *Ecotoxicology and Environmental Safety*. 2022;231:113160.
- [3]. Kul AR, Aldemir A, Alkan S, Elik H, Çalışkan M. Adsorption of Basic Blue 41 using Juniperus excelsa: kinetic, equilibrium and thermodynamic studies. *Environmental Research and Technology*. 2019;2(3):112–121.
- [4]. Regti A, Laamari MR, Stiriba S-E, El Haddad M. Removal of Basic Blue 41 dyes using Persea americana-activated carbon prepared by phosphoric acid action. *International Journal of Industrial Chemistry*. 2017;8(2):187–195.
- [5]. Gupta VK, Suhas, Mohan D. Equilibrium uptake and sorption dynamics for the removal of a basic dye (basic red) using low-cost adsorbents. *Journal of Colloid and Interface Science*. 2003;265(2):257–264.
- [6]. Goswami M, Phukan P. Enhanced adsorption of cationic dyes using sulfonic acid modified activated carbon. *Journal of Environmental Chemical Engineering*. 2017;5(4):3508–3517.
- [7]. Belala Z, Jeguirim M, Belhachemi M, Addoun F, Trouvé G. Biosorption of basic dye from aqueous solutions by date stones and palm-trees waste: kinetic, equilibrium and thermodynamic studies. *Desalination*. 2011;271(1–3):80–87.
- [8]. Aloud SS, Alharbi HA, Hameed BH, Giesy JP, Almady SS, Alotaibi KD. Production of activated carbon from date palm stones by hydrothermal carbonization and microwave-assisted KOH/NaOH activation for removal of dyes from wastewater. *Scientific Reports*. 2023;13:19064.
- [9]. Belhachemi M, Rios RVRA, Addoun F, Silvestre-Albero J, Sepúlveda-Escribano A, Rodríguez-Reinoso F. Preparation of activated carbon from date pits: effect of the activation agent and liquid-phase oxidation. *Journal of Analytical and Applied Pyrolysis*. 2009;86(1):168–172.
- [10]. Al-Qaessi F. Production of activated carbon from date stones by using zinc chloride. *Energy Sources, Part A: Recovery, Utilization, and Environmental Effects*. 2010;32(10):917–930.
- [11]. Hussein FH, Halbus AF, Lafta AJ, Athab ZH. Preparation and characterization of activated carbon from Iraqi Khestawy date palm. *Journal of Chemistry*. 2015;2015:295748.
- [12]. Ashour SS. Kinetic and equilibrium adsorption of methylene blue and remazol dyes onto steam-activated carbons developed from date pits. *Journal of Saudi Chemical Society*. 2010;14(1):47–53.
- [13]. Vadivelan V, Kumar KV. Equilibrium, kinetics, mechanism, and process design for the sorption of methylene blue onto rice husk. *Journal of Colloid and Interface Science*. 2005;286(1):90–100.

- [14]. Lagergren S. Zur theorie der sogenannten adsorption gelöster stoffe. Kungliga Svenska Vetenskapsakademiens Handlingar. 1898;24(4):1–39.
- [15]. Ho YS, McKay G. Pseudo-second order model for sorption processes. *Process Biochemistry*. 1999;34(5):451–465.
- [16]. Weber WJ Jr, Morris JC. Kinetics of adsorption on carbon from solution. *Journal of the Sanitary Engineering Division, ASCE*. 1963;89(2):31–59.
- [17]. Langmuir I. The adsorption of gases on plane surfaces of glass, mica and platinum. *Journal of the American Chemical Society*. 1918;40(9):1361–1403.
- [18]. Freundlich HMF. Über die adsorption in lösungen. *Zeitschrift für Physikalische Chemie*. 1906;57:385–470.
- [19]. Temkin MI, Pyzhev V. Kinetics of ammonia synthesis on promoted iron catalysts. *Acta Physicochimica URSS*. 1940;12:217–222.
- [20]. Dubinin MM, Radushkevich LV. The equation of the characteristic curve of activated charcoal. *Proceedings of the Academy of Sciences of the USSR, Physical Chemistry Section*. 1947;55:331–333.
- [21]. Pathania D, Sharma S, Singh P. Removal of methylene blue by adsorption onto activated carbon developed from *Ficus carica* bast. *Arabian Journal of Chemistry*. 2017;10:S1445–S1451.
- [22]. Bedin KC, Martins AC, Cazetta AL, Pezoti O, Almeida VC. KOH-activated carbon prepared from sucrose spherical carbon: adsorption equilibrium, kinetic and thermodynamic studies for methylene blue removal. *Chemical Engineering Journal*. 2016;286:476–484.
- [23]. Gougazeh M, Kooli F, Buhl JC. Removal efficiency of Basic Blue 41 by three zeolites prepared from natural Jordanian kaolin. *Clays and Clay Minerals*. 2019;67(2):143–153.
- [24]. Guemgam A, Gherbia A, Bakchiche B, Guenane H. Effect of treating activated carbon derived from date pits with H_2SO_4 on the adsorption of methylene blue. *Global NEST Journal*. 2025;27(5):1–13.
- [25]. Khadhri N, Saad MEK, Ben Mosbah M, Moussaoui Y. Batch and continuous column adsorption of indigo carmine onto activated carbon derived from date palm petiole. *Journal of Environmental Chemical Engineering*. 2019;7(1):102775.